

Next-to-Leading Order QCD Corrections to the Direct Top
Quark Production via Model-independent FCNC Couplings at
Hadron Colliders

Jian Jun Liu^{*}, Chong Sheng Li[†], and Li Lin Yang

Department of Physics, Peking University, Beijing 100871, China

Li Gang Jin

Institute of Theoretical Physics, Academia Sinica, Beijing 100080, China

(dated: January 26, 2020)

Abstract

We calculated the next-to-leading order (NLO) QCD corrections to the cross sections for direct top quark productions induced by model-independent FCNC couplings at hadron colliders. The NLO results increase the experimental sensitivity to the anomalous couplings. Our results show that the NLO QCD corrections enhance the leading order (LO) total cross sections at the Tevatron Run 2 about 60% for both of g_{tc}^g and g_{tu}^g couplings, and enhance the LO total cross sections at the LHC about 40% for g_{tc}^g couplings and 50% for g_{tu}^g couplings, respectively. Moreover, the NLO QCD corrections vastly reduce the dependence of the total cross sections on the renormalization or factorization scale, which leads to increased confidence in predictions based on these results.

PACS numbers: 14.65.Ha, 12.38.Bx, 12.60.Cn

^{*} Present address: Physics department, Tsinghua University, Beijing 100084, China; Electronics address:
liujj@mails.tsinghua.edu.cn

[†] Electronics address: csli@pku.edu.cn

I. INTRODUCTION

The flavor dynamics, such as the mixing of three generation fermions and their large mass differences observed, is still a great mystery in particle physics today. The heaviest one of three generation fermions is the top quark with the mass close to the electroweak (EW) symmetry breaking scale. Therefore, it can play a role of a wonderful probe for the EW breaking mechanism and new physics beyond the standard model (SM) through its decays and productions. An important aspect of the top quark physics is to investigate anomalous flavor changing neutral current (FCNC) couplings. Within the SM, the FCNC processes are forbidden at the tree-level and highly suppressed by the GIM mechanism [1] at one-loop level. All the current precise measurements of various FCNC processes, for example, $b \rightarrow s$ [2], agree with the SM predictions well. However, it should be noted that only few experimental constraints on the top quark FCNC processes are available so far, and many new physics models allow the existence of the tree-level FCNC couplings, and may greatly enhance some FCNC processes. Since the CERN Large Hadron Collider (LHC) can produce abundant top quark events, the measurement of the top quark rare processes will become possible. Therefore, a good understanding of the theoretical predictions of top quark FCNC processes is important for searching new physics.

Any new physics effect involved in top quark FCNC processes can be incorporated into an effective Lagrangian in a model independent way [3, 4]:

$$\begin{aligned}
 \mathcal{L}^e = & \frac{g}{2 \cos \theta_w} \sum_{q=u,c} \bar{t} (v_{tq}^Z + a_{tq}^Z \gamma_5) q Z + \frac{g}{2 \cos \theta_w} \sum_{q=u,c} \bar{t} (f_{tq}^Z + i h_{tq}^Z \gamma_5) q Z \\
 & + \sum_{q=u,c} \bar{e} \left(f_{tq}^A + i h_{tq}^A \gamma_5 \right) q A + g_s \sum_{q=u,c} \bar{t} \left(f_{tq}^g + i h_{tq}^g \gamma_5 \right) q G^a + \text{h.c.} \quad (1)
 \end{aligned}$$

where Λ is the new physics scale, θ_w is the Weinberg angle, and T^a are the Gell-Mann matrices satisfying $\text{Tr}(T^a T^b) = \delta^{ab} = 2$. The v_{tq}^Z, a_{tq}^Z can be complex in general, and $v_{tq}^Z = a_{tq}^Z = 0$ in the SM. $G^a = \frac{1}{\sqrt{2}} \lambda^a G^a = \frac{1}{\sqrt{2}} \lambda^a G^a = g_s f^{abc} G^b G^c$ and similarly for the other gauge bosons. Λ is normalized to be real and positive and f, h to be complex numbers satisfying for each term $|f|^2 + |h|^2 = 1$.

The top quark FCNC processes induced by various anomalous couplings have been studied in detail, for a most recent review, see [5]. In general, top quark decay processes provide the best place to discover top FCNC interactions involving anomalous $t \rightarrow q$ and $t \rightarrow q Z$ couplings. However, for $t \rightarrow q g$ anomalous couplings, i.e., the forth term in Equ.(1), the best

processes are the top quark FCNC productions [6, 7], and the direct top quark production processes are the most sensitive ones [7]. The current constraints on the top quark anomalous couplings are $\frac{g_{tq}}{\Lambda^2} = 0.47 \text{ TeV}^{-2}$ [8], and as pointed out in [4, 7] based on tree-level analysis of the direct top quark productions, the couplings can further be detected down to $\frac{g_{tc}}{\Lambda^2} = 0.0084 \text{ TeV}^{-2}$, $\frac{g_{tu}}{\Lambda^2} = 0.0033 \text{ TeV}^{-2}$ at the LHC, and $\frac{g_{tc}}{\Lambda^2} = 0.062 \text{ TeV}^{-2}$, $\frac{g_{tu}}{\Lambda^2} = 0.019 \text{ TeV}^{-2}$ at the Tevatron Run 2. However, since these processes involve strongly interacting particles in their initial states and final states, the lowest order results in general have large theoretical uncertainties. In this paper, we present the complete NLO QCD calculation for the cross section of direct top quark productions induced by model-independent FCNC couplings at hadron colliders.

The arrangement of this paper is as follows. In Sec. II we show the LO results. In Sec. III we present the details of the NLO calculations including the virtual and real corrections. In Sec. IV by a numerical analysis we present the predictions for total cross sections at hadron colliders.

II. THE LEADING ORDER RESULTS

We start from the flavor-changing operators including top quark anomalous couplings:

$$g_s \sum_{q=u,c} \frac{g_{tq}}{\Lambda^2} \bar{t} T^a (F_{tq}^g + i h_{tq}^g \gamma_5) q G^a + \text{h.c.}; \quad (2)$$

and consider the leading order (LO) scattering process of hadrons P_1 and P_2 to top quark:

$$P_1(p_1) + P_2(p_2) \rightarrow g(k_1) + q(k_2) \rightarrow t(p_t) + X; \quad q = c \text{ or } u; \quad (3)$$

The spin and color averaged squared matrix element is

$$\overline{|\mathcal{M}^B|^2} = \frac{8}{3} \frac{s}{\Lambda^4} \frac{g_{tq}^2}{\Lambda^4} m_t^4; \quad (4)$$

which, after the phase space integration, gives the LO partonic cross section (the masses of charm quark and up quark are neglected)

$$\hat{\sigma}^B(z) = \frac{8}{3} \frac{s}{\Lambda^4} \frac{g_{tq}^2}{\Lambda^4} m_t^2 (1-z); \quad (5)$$

where $s = (k_1 + k_2)^2$ and $z = m_t^2/s$. The LO total cross section at hadron colliders is obtained by convoluting the partonic cross section with the parton distribution functions

(PDFs) $G_{g,P}$ in the proton (anti-proton):

$$G_{g,P}^B = \int dx_1 dx_2 [G_{g=P_1}(x_1; F) G_{q=P_2}(x_2; F) + (x_1 \leftrightarrow x_2)]^B; \quad (6)$$

where F is the factorization scale.

III. THE NEXT-TO-LEADING ORDER CALCULATIONS

For convenience, in this section we only present the results for $gc \rightarrow t$, and the ones for $gu \rightarrow t$ can be obtained by replacing c with u in related formulas. The cross sections beyond LO involve the computation of one loop virtual gluon corrections (Figs.1 (v₁)-(v₁₂)) and real gluon bremsstrahlung contributions to leading order processes (Figs.2 (r₁)-(r₆)). We also include processes with two gluons in the initial states (Figs.2 (g₁)-(g₄)) as well as two quarks in the initial states (Figs.2 (s₁)-(s₃)). We will encounter ultraviolet (UV) and infrared (IR) (soft and collinear) divergences in our computation. We have used $n = 4 - 2\epsilon$ dimensional regularization [9] to regulate both these divergences, and all divergences appear as $1/\epsilon$ with $\epsilon = 1/2$.

The virtual corrections to direct top productions consist of self-energy and vertex diagrams, which represent the QCD corrections arising from quarks and gluons. The total virtual amplitude contains UV and IR divergences (the imaginary part is neglected):

$$M^{\text{virt}} = \frac{s}{12} C \left[\frac{13}{2} \frac{1}{\text{IR}} - \frac{17}{\text{IR}} + \frac{11}{\text{UV}} + \frac{17}{3} \frac{1}{\epsilon} \right] M^B + \frac{1}{2} Z_2^{(g)} + \frac{1}{2} Z_2^{(c)} + \frac{1}{2} Z_2^{(t)} + Z_{g_s} + Z_{g_{tc}} M^B; \quad (7)$$

where $C = (1 + \frac{2}{3}) \frac{4}{m_t^2}$, and the UV divergences are renormalized by introducing counterterms for the wave function of the external fields ($Z_2^{(g)}$, $Z_2^{(c)}$, $Z_2^{(t)}$), and the coupling constants (Z_{g_s} , $Z_{g_{tc}}$). We define these counterterms according to the following convention. For the external fields, we fix $Z_2^{(g)}$, $Z_2^{(c)}$ and $Z_2^{(t)}$ using on-shell subtraction, and, therefore, they also have IR singularities:

$$\begin{aligned} Z_2^{(g)} &= \frac{s}{2} C \left[\frac{n_f}{3} - \frac{5}{2} \frac{1}{\text{UV}} - \frac{1}{\text{IR}} - \frac{s}{6} C \frac{1}{\text{UV}} \right]; \\ Z_2^{(c)} &= \frac{s}{3} C \left[\frac{1}{\text{UV}} - \frac{1}{\text{IR}} \right]; \\ Z_2^{(t)} &= \frac{s}{3} C \left[\frac{1}{\text{UV}} + \frac{2}{\text{IR}} + 4 \right]; \end{aligned} \quad (8)$$

where $n_f = 5$. For the renormalization of g_s , we use the $\overline{\text{MS}}$ scheme modified to decouple the top quark [10], i.e. the first n_f light flavors are subtracted using the $\overline{\text{MS}}$ scheme, while the divergences associated with the top-quark loop are subtracted at zero momentum:

$$Z_{g_s} = \frac{s}{4} (1 + \dots) (4 - \dots) \left(\frac{n_f}{3} - \frac{11}{2} \right) \frac{1}{\mu_{UV}} + \frac{s}{12} C \frac{1}{\mu_{UV}} : \quad (9)$$

Thus, in this scheme, the renormalized strong coupling constant g_s evolves with n_f light flavors. Finally, for $Z_{g_{tc=}}$, we adopt the $\overline{\text{MS}}$ scheme and adjust it to cancel the remaining UV divergences exactly:

$$Z_{g_{tc=}} = \frac{s}{6} (1 + \dots) (4 - \dots) \frac{1}{\mu_{UV}} : \quad (10)$$

Therefore, now M^{virt} has no UV-singular contributions.

The partonic cross section of real gluon bremsstrahlung are:

$$\begin{aligned} \hat{\sigma}^{\text{real}}(z; 1 = \text{IR}) = & \frac{4}{9s} \frac{s^2}{m_t^2} \frac{g_{tc=}^2}{m_t^2} C^0 \left[\frac{13}{2} \frac{1}{\text{IR}} + \frac{4}{\text{IR}} (1-z) + \frac{1}{\text{IR}} (18z^2 - 14z + 40) \frac{18}{z} \right. \\ & \left. + \frac{26}{(1-z)_+} + 8(1-z) + \frac{1}{8(1-z)_+} (27z^2 - 57z - 2(77z + 27) \ln z - 23) \right. \\ & \left. + \frac{11}{z} + \frac{77z + 27}{2} \frac{\ln(1-z)}{1-z} + 36z^2 - 28z + \frac{83}{2} - \frac{36}{z} \ln(1-z) \right. \\ & \left. + 28z^2 - 22z + \frac{107}{4} - \frac{18}{z} - \frac{2}{1-z} \ln z + 14z^2 - \frac{73z}{8} + \frac{63}{4} - \frac{109}{8z} \right] ; \quad (11) \end{aligned}$$

where $C^0 = \frac{(1-z)}{(1-z)^2} \frac{4}{m_t^2} s^2$. The "plus" functions appearing in the above results are the distributions which satisfy the following equation

$$\int_0^1 dz f_+(z) g(z) = \int_0^1 dz f(z) g(z) - g(1) ; \quad (12)$$

where $g(z)$ is any well-behaved function in the region $0 \leq z \leq 1$.

Combining the contributions of the LO result, the virtual corrections and the real gluon bremsstrahlung, we obtain the bare NLO partonic cross section:

$$\begin{aligned} \hat{\sigma}_{\text{gc}}^{\text{bare}}(z; 1 = \text{IR}) = & \frac{8}{3s} \frac{s^2}{m_t^2} \frac{g_{tc=}^2}{m_t^2} (1-z) \\ & + \frac{4}{9s} \frac{s^2}{m_t^2} \frac{g_{tc=}^2}{m_t^2} C^0 \left[\frac{3}{\text{IR}} - 2N_c \left(\frac{z}{(1-z)_+} + \frac{1}{z} + z \ln(1-z) \right) \right] \end{aligned}$$

$$\begin{aligned}
& \frac{11}{2} \frac{n_f}{3} (1-z) \frac{4}{3} \frac{1+z^2}{(1-z)_+} + \frac{3}{2} (1-z) + \frac{4}{3} \frac{z^2}{3} \quad 15 \\
& n_f \frac{29}{2} \ln \frac{z}{m_t^2} (1-z) + \frac{1}{8(1-z)_+} 27z^2 - 57z - 2(77z+27) \ln z \\
& 23 \frac{11}{z} + \frac{77z+27}{2} \frac{\ln(1-z)}{1-z} + 36z^2 - 28z + \frac{83}{2} \frac{36}{z} \ln(1-z) \\
& + 28z^2 - 22z + \frac{107}{4} \frac{18}{z} \frac{2}{1-z} \ln z + 14z^2 - \frac{73z}{8} + \frac{63}{4} \frac{109}{8z} ; \quad (13)
\end{aligned}$$

where $N_c = 3$. Now the soft divergences coming from virtual gluons and bremsstrahlung contributions have cancelled exactly according to the Bloch-Nordsieck theorem [11]. The remaining divergences are collinear.

Moreover, calculating the processes with two gluons or two light quarks in the initial states, we obtain the following partonic cross sections

$$\begin{aligned}
\hat{\sigma}_{gg}^{\text{bare}}(z; 1=_{\text{IR}}) &= \frac{8}{3s} \frac{s}{m_t^2} \frac{g_{tc}^2}{m_t^2} C_0 \frac{z^2 + (1-z)^2}{2} \frac{1}{\text{IR}} + \frac{z^2}{4} + \frac{17z}{8} \frac{1}{4(1+z)} \\
&+ \frac{3}{8} \ln z + (2z^2 - 2z + 1) \ln(1-z) - \frac{259}{64} z^2 + \frac{505}{128} z + \frac{1}{16} + \frac{5}{128z} ;
\end{aligned}$$

$$\begin{aligned}
\hat{\sigma}_{cc}^{\text{bare}}(z; 1=_{\text{IR}}) &= \frac{32}{9s} \frac{s}{m_t^2} \frac{g_{tc}^2}{m_t^2} C_0 \frac{1 + (1-z)^2}{z} \frac{1}{\text{IR}} + 2z \ln(1-z) - z \ln z \\
&4 \ln(1-z) + 2 \ln z + \frac{10}{3} + \frac{4}{z} \ln(1-z) - \frac{2}{z} \ln z - \frac{7}{3z} ;
\end{aligned}$$

$$\begin{aligned}
\hat{\sigma}_{cc}^{\text{bare}}(z; 1=_{\text{IR}}) &= \frac{16}{9s} \frac{s}{m_t^2} \frac{g_{tc}^2}{m_t^2} C_0 \frac{1 + (1-z)^2}{z} \frac{1}{\text{IR}} + 2z \ln(1-z) - z \ln z \\
&\frac{2}{3} z - 4 \ln(1-z) + 2 \ln z - \frac{4}{3z} + \frac{7}{3} + \frac{4}{z} \ln(1-z) - \frac{2}{z} \ln z + \frac{2}{3} z^2 ;
\end{aligned}$$

$$\begin{aligned}
\hat{\sigma}_{cq(q)}^{\text{bare}}(z; 1=_{\text{IR}}) &= \frac{16}{9s} \frac{s}{m_t^2} \frac{g_{tc}^2}{m_t^2} C_0 \frac{1 + (1-z)^2}{z} \frac{1}{\text{IR}} + 2z \ln(1-z) - z \ln z \\
&4 \ln(1-z) + 2 \ln z + 3 + \frac{4}{z} \ln(1-z) - \frac{2}{z} \ln z - \frac{2}{z} ;
\end{aligned}$$

$$\hat{\sigma}_{qq}(z) = \frac{16}{9s} \frac{s}{m_t^2} \frac{g_{tc}^2}{m_t^2} \frac{2}{3} z^2 - z + \frac{1}{3z} ; \quad (14)$$

Note that the divergences appearing in above expressions are collinear, and the partonic cross section of $q\bar{q}(q\bar{c})$ initial state is free of singularities.

The bare partonic cross sections in Eqs. (13) and (14), which contain the collinear singularities generated by the radiation of gluons and massless quarks, have a universal structure, and can be factorized into the following form to all orders of perturbation theory:

$$\hat{\sigma}_{ab}^{\text{bare}}(z; 1=_{\text{IR}}) = \sum_{c;d} \sigma_{ca}(z; F; 1=_{\text{IR}}) \otimes \sigma_{db}(z; F; 1=_{\text{IR}}) \hat{\sigma}_{cd}(z; F); \quad (15)$$

where F is the factorization scale and \otimes is the convolution symbol defined as

$$f(z) \otimes g(z) = \int_z^1 \frac{dy}{y} f(y) g\left(\frac{z}{y}\right); \quad (16)$$

The universal splitting functions $\sigma_{cd}(z; F; 1=_{\text{IR}})$ represent the probability of finding a particle c with fraction z of the longitudinal momentum inside the parent particle d at the scale F . They contain the collinear divergences, and can be absorbed into the redefinition of the PDF according to mass factorization [12]. Adopting the $\overline{\text{MS}}$ mass factorization scheme, we have to $\mathcal{O}(\epsilon_s)$

$$\sigma_{cd}(z; F; 1=_{\text{IR}}) = \sigma_{cd}(1-z) \frac{1}{2} \frac{s}{(1-z)} \left(\frac{1}{2}\right) \frac{4}{F^2} P_{cd}^{(0)}(z); \quad (17)$$

where $P_{cd}^{(0)}(z)$ are the leading order Altarelli-Parisi splitting functions [13]:

$$\begin{aligned} P_{qq}^{(0)}(z) &= \frac{4}{3} \frac{1+z^2}{(1-z)_+} + \frac{3}{2} (1-z); \\ P_{qg}^{(0)}(z) &= \frac{1}{2} (1-z)^2 + z^2; \\ P_{gq}^{(0)}(z) &= \frac{4}{3} \frac{(1-z)^2 + 1}{z}; \\ P_{gg}^{(0)}(z) &= 2N_c \frac{z}{(1-z)_+} + \frac{1}{z} + z(1-z) + \frac{11}{2} \frac{n_f}{3} (1-z); \end{aligned} \quad (18)$$

After absorbing the splitting functions $\sigma_{cd}(z; F; 1=_{\text{IR}})$ into the redefinition of the PDFs through the mass factorization in this way, we have the hard scattering cross sections $\hat{\sigma}_{ab}(z; F)$, which are free of collinear divergences, and depend on the scale F :

$$\hat{\sigma}_{gc}(z; F) = \frac{8}{3s} \frac{g^2}{m_t^2} (1-z)$$

$$\begin{aligned}
& + \frac{4}{9s} \frac{g_{tc}^2}{m_t^2} \left(3 \ln \frac{m_t^2}{2F} 2N_c \frac{z}{(1-z)_+} + \frac{1}{z} + z(1-z) \right) \\
& + \frac{11}{2} \frac{n_f}{3} (1-z) + \frac{4}{3} \frac{1+z^2}{(1-z)_+} + \frac{3}{2} (1-z) + \frac{4}{3} \quad 15 \\
& n_f \frac{29}{2} \ln \frac{r}{m_t^2} (1-z) + \frac{1}{8(1-z)_+} 27z^2 - 57z - 2(77z+27) \ln z \\
& 23 \frac{11}{z} + \frac{77z+27}{2} \frac{\ln(1-z)}{1-z} + 36z^2 - 28z + \frac{83}{2} - \frac{36}{z} \ln(1-z) \\
& + 28z^2 - 22z + \frac{107}{4} - \frac{18}{z} - \frac{2}{1-z} \ln z + 14z^2 - \frac{73z}{8} + \frac{63}{4} - \frac{109}{8z} ; \\
\hat{\sigma}_{gg}(z; F) & = \frac{8}{3s} \frac{g_{tc}^2}{m_t^2} \ln \frac{m_t^2}{2F} \frac{z^2 + (1-z)^2}{2} + \frac{z^2}{4} + \frac{17z}{8} - \frac{1}{4(1+z)} \\
& + \frac{3}{8} \ln z + (2z^2 - 2z + 1) \ln(1-z) - \frac{259}{64} z^2 + \frac{505}{128} z + \frac{1}{16} + \frac{5}{128z} ; \\
\hat{\sigma}_{cc}(z; F) & = \frac{32}{9s} \frac{g_{tc}^2}{m_t^2} \ln \frac{m_t^2}{2F} \frac{1 + (1-z)^2}{z} + 2z \ln(1-z) - z \ln z \\
& 4 \ln(1-z) + 2 \ln z + \frac{10}{3} + \frac{4}{z} \ln(1-z) - \frac{2}{z} \ln z - \frac{7}{3z} ; \\
\hat{\sigma}_{cc}(z; F) & = \frac{16}{9s} \frac{g_{tc}^2}{m_t^2} \ln \frac{m_t^2}{2F} \frac{1 + (1-z)^2}{z} + 2z \ln(1-z) - z \ln z \\
& \frac{2}{3} z - 4 \ln(1-z) + 2 \ln z - \frac{4}{3z} + \frac{7}{3} + \frac{4}{z} \ln(1-z) - \frac{2}{z} \ln z + \frac{2}{3} z^2 ; \\
\hat{\sigma}_{c\bar{q}(q)}(z; F) & = \frac{16}{9s} \frac{g_{tc}^2}{m_t^2} \ln \frac{m_t^2}{2F} \frac{1 + (1-z)^2}{z} + 2z \ln(1-z) - z \ln z \\
& 4 \ln(1-z) + 2 \ln z + 3 + \frac{4}{z} \ln(1-z) - \frac{2}{z} \ln z - \frac{2}{z} ; \tag{19}
\end{aligned}$$

Finally, we combine these finite $\hat{\sigma}_{ab}(z; F)$ with the appropriate partonic distribution functions to arrive at the NLO cross sections for the direct top productions:

$$\sigma^{NLO} = \int dx_1 dx_2 \sum_{g=P_1}^h G_{g=P_1}(x_1; F) \sum_{c=P_2}^i G_{c=P_2}(x_2; F) + (x_1 \leftrightarrow x_2) \hat{\sigma}_{gc}(z; F)$$

$$\begin{aligned}
& + G_{g=P_1}(\mathbf{x}_1; F)G_{g=P_2}(\mathbf{x}_2; F)\hat{\sigma}_{gg}(z; F) + G_{c=P_1}(\mathbf{x}_1; F)G_{c=P_2}(\mathbf{x}_2; F)\hat{\sigma}_{cc}(z; F) \\
& + G_{c=P_1}^h(\mathbf{x}_1; F)G_{c=P_2}(\mathbf{x}_2; F) + G_{c=P_1}^i(\mathbf{x}_1, \mathbf{x}_2)\hat{\sigma}_{cc}(z; F) \\
& + \sum_{q(q)} G_{c=P_1}^h(\mathbf{x}_1; F)G_{q(q)=P_2}(\mathbf{x}_2; F) + G_{c=P_1}^i(\mathbf{x}_1, \mathbf{x}_2)\hat{\sigma}_{cq(q)}(z; F) : \tag{20}
\end{aligned}$$

IV. NUMERICAL CALCULATION AND DISCUSSION

In this section, we present the numerical results of the NLO QCD corrections to the direct top quark production via anomalous FCNC couplings at the Tevatron Run 2 ($\sqrt{s} = 2.0 \text{ TeV}$) and the LHC ($\sqrt{s} = 14 \text{ TeV}$). In our numerical calculations, we take the top quark mass $m_t = 178.0 \text{ GeV}$ [14] and the two-loop evolution of $\alpha_s(\mu_r)$ [15] with $\alpha_s(M_Z) = 0.118$. Moreover, CTEQ6L (CTEQ6M) PDFs [16] are used in the calculation of the LO (NLO) cross sections. As for the anomalous couplings, which appear in the expressions as quadratic factors, we choose $\frac{g}{\Lambda^2} = 0.01 \text{ TeV}^{-2}$.

In Table I, we list the LO and NLO cross sections for the center value of the factorization and renormalization scale $\mu_F = \mu_r = m_t$. One can see that for $gc \rightarrow t$ ($gu \rightarrow t$), the NLO predictions enhance the LO results 61% (59%) at the Tevatron Run 2, and the 40% (52%) at the LHC, respectively.

Fig.3 shows the LO and NLO cross sections as functions of factorization (renormalization) scales for subprocesses $gc \rightarrow t$ and $gu \rightarrow t$ at the Tevatron Run 2. The K factor is defined as the ratio of the LO and NLO cross sections to their values at $\mu_F = \mu_r = m_t$. For each subprocess, we show the scale dependence for three cases: (1) μ_F and μ_r varies simultaneously, (2) $\mu_F = m_t$ and only μ_r varies, (3) $\mu_r = m_t$ and only μ_F varies. We can find that for the three cases, the NLO QCD corrections remarkably reduce the dependence of theoretical predictions on the factorization (renormalization) scales. For example, in the region $m_t=2 \mu_F = \mu_r = 2m_t$, the cross sections vary by 18% at LO but by 11% at NLO for $gu \rightarrow t$, and vary by 15% at LO but by 9% at NLO for $gc \rightarrow t$.

Fig.4 shows the LO and NLO cross sections as functions of factorization (renormalization) scales at the LHC. One can find that the scale dependence is reduced after considering the NLO QCD corrections in case (2) and (3). For case (1), although the NLO results show the weaker scale dependence when $\mu_F = \mu_r$ is large ($\gg m_t$), the NLO results do not reduce the

subprocess	LHC (LO)	LHC (NLO)	Tevatron Run 2 (LO)	Tevatron Run 2 (NLO)
$g_u \rightarrow t$	11069.8	16817.8	259.0	412.6
$g_c \rightarrow t$	1817.1	2536.6	17.6	28.3

TABLE I: The LO and NLO cross sections of direct top quark production via anomalous FCNC couplings at the LHC and Tevatron Run 2 (fb). Here $\frac{g}{\Lambda^2} = 0.01 \text{ TeV}^{-2}$ and $\mu_F = \mu_R = m_t$.

scale dependence of theoretical predictions for $\mu_F = \mu_R = m_t$. The main origins to the scale dependence come from the terms proportional to $(1-z)$ in $\hat{\sigma}_{gc}(z; \mu_F)$, and higher order effects are necessary to further reduce such scale dependence in the case of $\mu_F = \mu_R$ at the LHC. Similar phenomena also can be found in other processes [17].

V. CONCLUSIONS

We have calculated the NLO QCD corrections to the cross sections for direct top quark productions induced by model-independent FCNC couplings at hadron colliders. The NLO results increase the experimental sensitivity to the anomalous couplings. Our results show that the NLO QCD corrections enhance the LO total cross sections at the Tevatron Run 2 about 60% for both of $\frac{g}{\Lambda^2}$ and $\frac{g}{\Lambda^2}$ couplings, and enhance the LO total cross sections at the LHC about 40% for $\frac{g}{\Lambda^2}$ couplings and 50% for $\frac{g}{\Lambda^2}$ couplings, respectively. Moreover, the NLO QCD corrections vastly reduce the dependence of the total cross sections on the renormalization or factorization scale, which leads to increased confidence in predictions based on these results.

Acknowledgments

We would like to thank C.-P. Yuan and T. Han for useful discussions. This work was supported in part by the National Natural Science Foundation of China, Specialized Research Fund for the Doctoral Program of Higher Education and China Postdoctoral Science

Foundation.

- [1] S.L. Glashow, J. Iliopoulos, and L. Maiani, *Phys. Rev. D* **2**, 1285 (1970).
- [2] S. Eidelman et al, *Phys. Lett. B* **592**, 1 (2004).
- [3] W. Hollik, J.I. Illana, S. Rigolin, C. Schappacher, and D. Stockinger, *Nucl. Phys. B* **551**, 3 (1999); *Nucl. Phys. B* **557**, 407 (E) (1999).
- [4] M. Beneke et al, hep-ph/0003033.
- [5] J.A. Aguilar-Saavedra, *Acta Phys. Polon. B* **35**, 2695 (2004).
- [6] E. Malkawi and T. Tait, *Phys. Rev. D* **54**, 5758 (1996); T. Han, M. Hosh, K. Whisnant, B.-L. Young, and X. Zhang, *Phys. Rev. D* **58**, 073008 (1998); Y.P. Gouz and S.R. Slabospitsky, *Phys. Lett. B* **457**, 177 (1999); A. Belyaev and N. Kidonakis, *Phys. Rev. D* **65**, 037501 (2002).
- [7] M. Hosh, K. Whisnant, and B.-L. Young, *Phys. Rev. D* **56**, 5725 (1997).
- [8] Y.P. Gouz and S.R. Slabospitsky, *Phys. Lett. B* **457**, 177 (1999).
- [9] G. 't Hooft and M. Veltman, *Nucl. Phys. B* **44**, 189 (1972).
- [10] J. Collins, F. Wilczek, and A. Zee, *Phys. Rev. D* **18**, 242 (1978).
- [11] F. Bloch and A. Nordsieck, *Phys. Rev.* **52**, 54 (1937).
- [12] J.C. Collins, D.E. Soper, and G. Sterman, *Nucl. Phys. B* **261**, 104 (1985); *Phys. Rev. D* **31**, 2616 (1985); *Phys. Rev. D* **34**, 3932 (E) (1986).
- [13] G. Altarelli and G. Parisi, *Nucl. Phys. B* **126**, 298 (1977).
- [14] D0 Collaborations, *Nature* **429**, 638 (2004).
- [15] S.G. Gorshny, A.L. Kataev, S.A. Larin, and L.R. Surguladze, *Mod. Phys. Lett. A* **5**, 2703 (1990); *Phys. Rev. D* **43**, 1633 (1991); A. Djouadi, M. Spira, and P.M. Zerwas, *Z. Phys. C* **70**, 427 (1996); A. Djouadi, J. Kalinowski, and M. Spira, *Comput. Phys. Commun.* **108**, 56 (1998); M. Spira, *Fortschr. Phys.* **46**, 203 (1998).
- [16] J. Pumplin, D.R. Stump, J. Huston, H.L. Lai, P. Nadolsky, and W.K. Tung, *J. High Energy Phys.* **0207** (2002) 012.
- [17] For example, see: J. Ohnemus, *Phys. Rev. D* **47**, 940 (1993); S. Dawson and R.P. Kauffman, *Phys. Rev. D* **49**, 2298 (1994); R.J. Gonsalves, N. Kidonakis, and A.S. Vera, hep-ph/0507317.

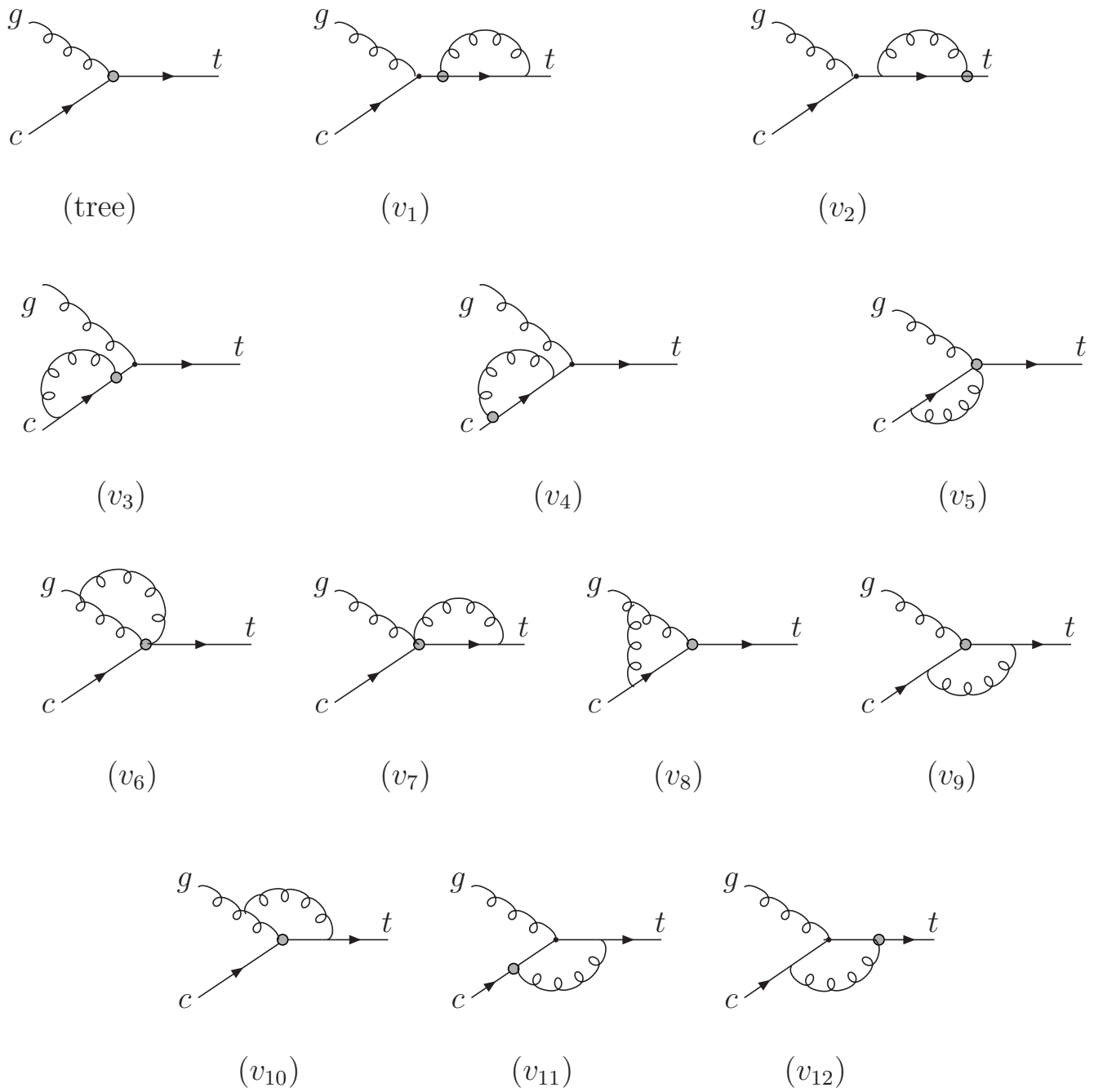


FIG . 1: Tree-level and one-loop Feynman diagrams for the direct top quark production .

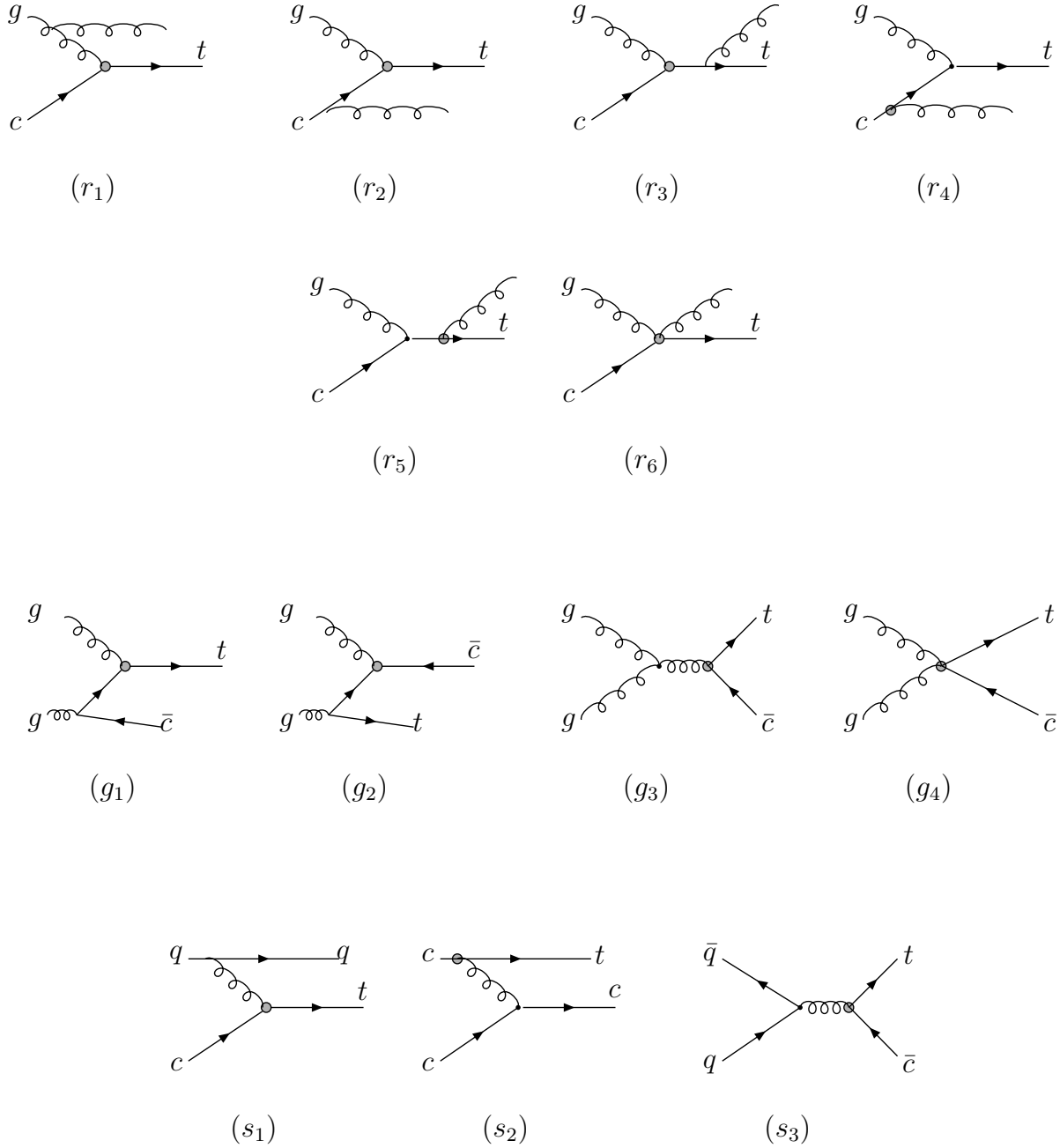


FIG . 2: Feynman diagrams of real gluon emission subprocesses ($(r_1) \dots (r_6)$), gluon initial state subprocesses ($(g_1) \dots (g_4)$), of which (g_1) and (g_2) have cross diagrams, and quark initial state subprocesses ($(s_1) \dots (s_3)$), of which (s_2) has cross diagram .

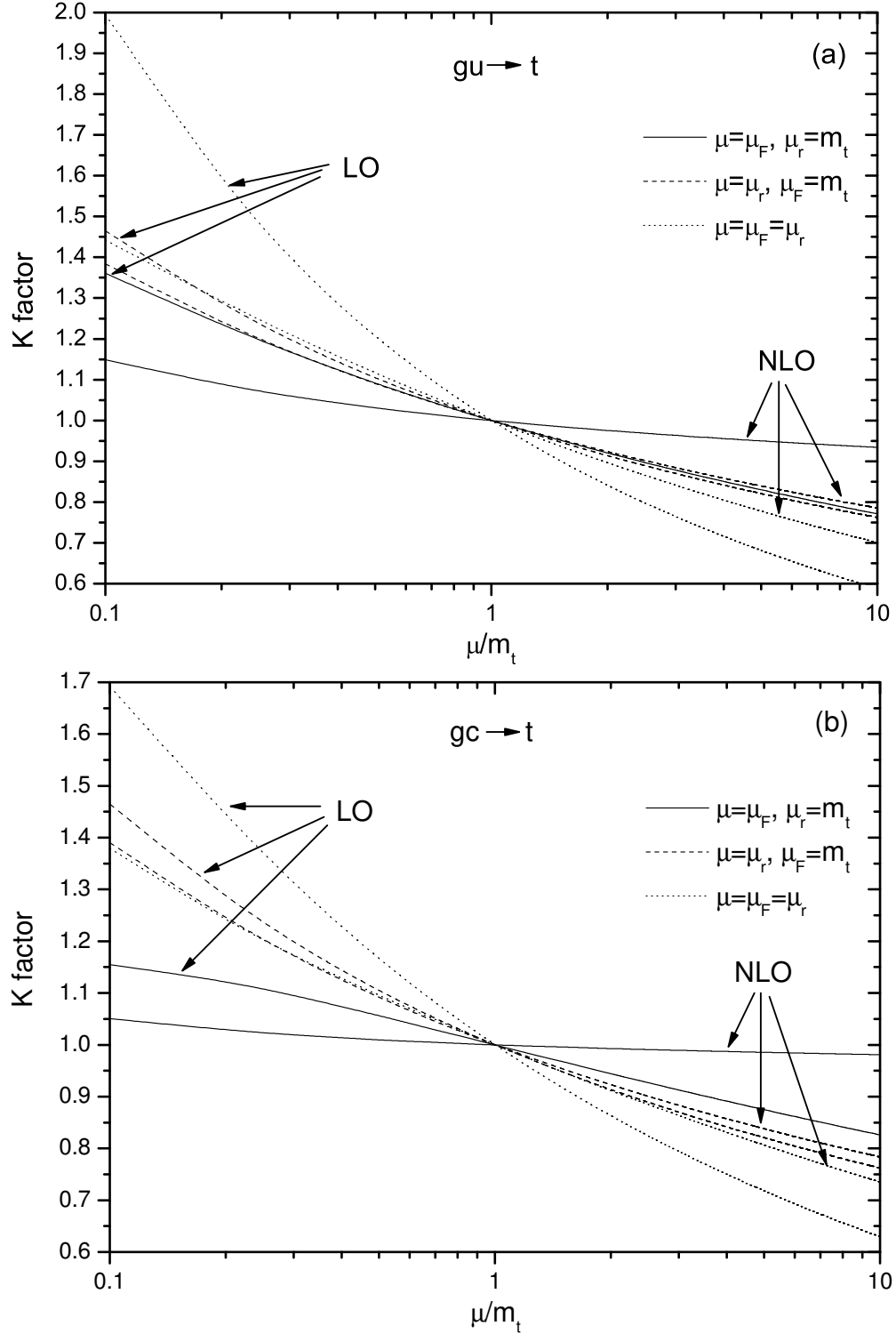


FIG . 3: The LO and NLO cross sections of direct top quark productions at Tevatron Run 2 and their dependence on the factorization/renormalization scales: (a) up quark initial state and (b) charm quark initial state. Here $\frac{g_{tc(u)}}{m_t} = 0.01 \text{TeV}^{-1}$.

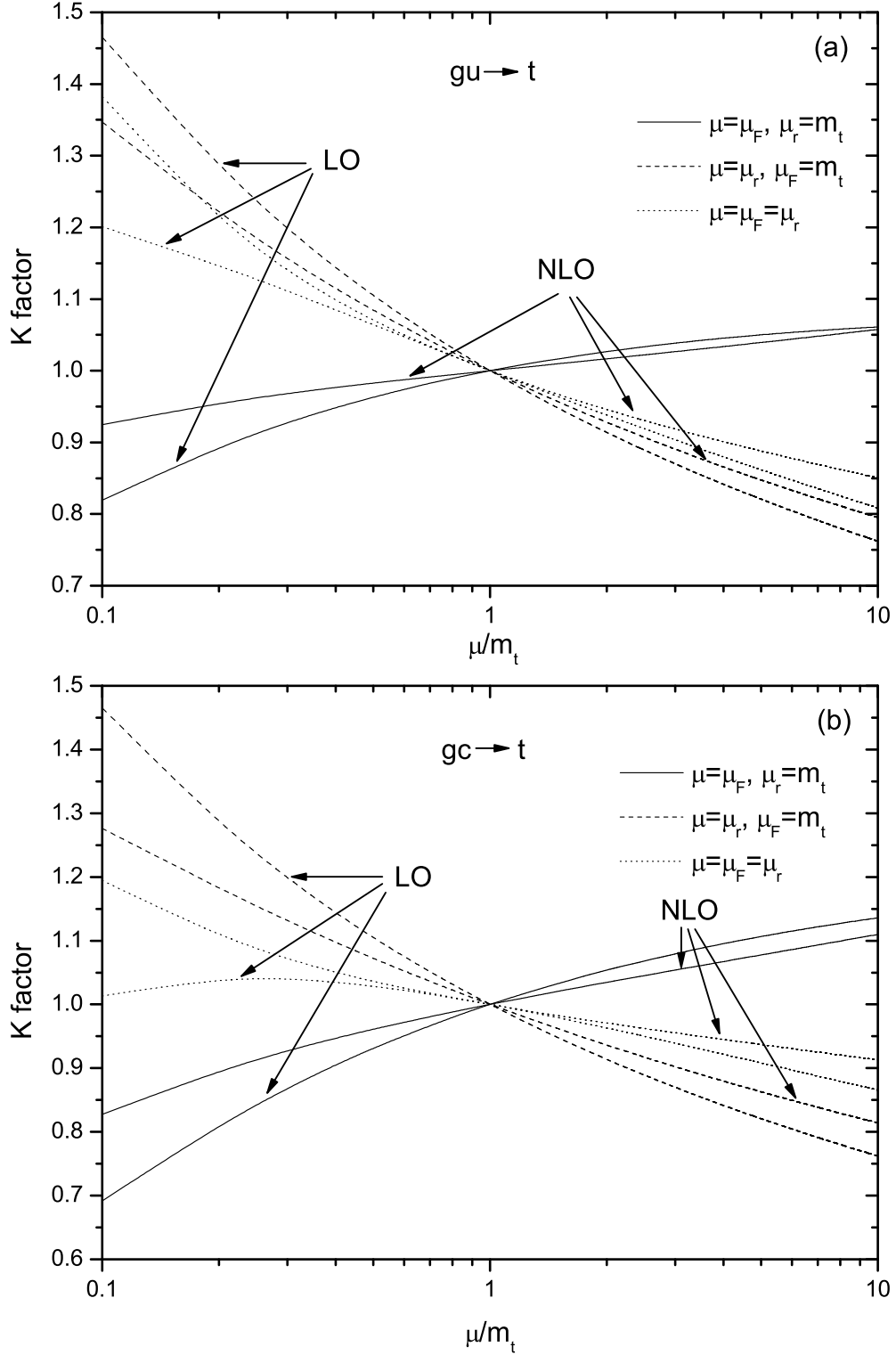


FIG . 4: The LO and NLO cross sections of direct top quark productions at the LHC and their dependence on the factorization/renormalization scales: (a) up quark initial state and (b) charm quark initial state. Here $\frac{\alpha_s}{4\pi} = 0.01 \text{TeV}^{-1}$.